Green Chemistry

PAPER

View Article Online
View Journal

Cite this: DOI: 10.1039/c6gc00977h

A study of poplar organosolv lignin after melt rheology treatment as carbon fiber precursors

Qining Sun,[a,b] Ratayakorn Khunsupat,[a] Kokouvi Akato,[c] Jingming Tao,[d] Nicole Labbé,*[d] Nidia C. Gallego,[c] Joseph J. Bozell,[d] Timothy G. Rials,[d] Gerald A. Tuskan,[e] Timothy J. Tschaplinski,[e] Amit K. Naskar,*[c] Yunqiao Pu[f] and Arthur J. Ragauskas*[a,f,g]

Received 7th April 2016,
Accepted 31st May 2016

DOI: 10.1039/c6gc00977h

www.rsc.org/greenchem

Lignins from various poplar genotypes were isolated by using organosolv fractionation and subjected to rheological treatment at various temperatures. Physicochemical characterization of the lignin variants shows a broad distribution of glass transition temperatures, melt viscosity, and pyrolysis char residues. Rheological treatment at 170 °C induces lignin repolymerization accompanied with an increase in condensed linkages, molecular weights, and viscosities. In contrast, rheology testing at 190 °C results in the decrease in lignin aliphatic and phenolic hydroxyl groups, β-O-aryl ether linkages, molecular weights, and viscosity values. Lignin under air cooling generates more oxygenated and condensed compounds, but lower amounts of ether linkages than lignin cooled under nitrogen. Lignin with a lower syringyl/guaiacyl ratio tends to form more cross-linkages along with higher viscosity values, higher molecular weight and larger amounts of condensed bonds.

Introduction

Carbon fibers are among the most important engineered materials for a variety of industrial applications due to their unique properties, including high stiffness and tensile strength, low thermal expansion and density, heat tolerance and reagent resistance. However, the main barriers to the large-scale production of commercial products are the high cost of petroleum-based carbon fiber precursors polyacrylonitrile (PAN) and the associated processing costs.[1] In an effort to address these barriers, lignin as an alternative precursor with low cost draws significant attention to the potential manufacturing of carbon fiber.[2] Nonetheless, to date, lignin based carbon fibers do not offer mechanical properties required for many structural applications. Several factors have been proposed to impair the physical properties of lignin carbon fiber, including structural heterogeneity, impurities and isolation methods.[3] Current methods for manufacturing carbon fiber from lignin involve isolation/purification of lignin, melt fiber spinning, oxidative thermo-stabilization, carbonization, graphitization and surface treatment.[4a] Recently, Mainka *et al.* characterized major reactions during the conversion of lignin to carbon fiber by using nuclear magnetic resonance (NMR) spectroscopy and Fourier transform infrared (FTIR) spectroscopy and reaction mechanisms were proposed.[4b] However, understanding on thermal behaviors and lignin chemistry during lignin melt treatment is still very limited. In an effort to increase the strength and integrity of lignin fibers during oxidative thermo-stabilization and subsequent downstream processing, it is essential to understand changes of the thermo-rheological properties of lignin and its associated chemical structures during thermal treatment. Such an understanding would facilitate the improvement in lignin derived carbon fibers. This study focuses on exploring lignin structural features and the associated chemistry under thermal and mechanical deformation after a melt rheological treatment.

Lignin is one of the most abundant natural biopolymers that accounts for 10–30 wt% of plant cell walls. It is a complex substituted polyphenol derived typically from hydroxycinnamyl monolignols (*i.e.*, coniferyl alcohol, sinapyl alcohol, and *para*-coumaryl alcohol) with different degrees of methoxylation. The polymerization of these monolignols in native biomass

[a]*School of Chemistry and Biochemistry, Renewable Bioproducts Institute, Georgia Institute of Technology, Atlanta, GA 30332, USA. E-mail: aragausk@utk.edu*
[b]*Department of Chemical and Biomolecular Engineering, University of Tennessee, Knoxville, TN 37996-2200, USA*
[c]*Carbon & Composites Group, Oak Ridge National Laboratory, Oak Ridge, Tennessee 37831-6053, USA. E-mail: naskarak@ornl.gov*
[d]*Center for Renewable Carbon, University of Tennessee Institute of Agriculture, Knoxville, TN 37996, USA. E-mail: nlabbe@utk.edu*
[e]*Biosciences Division, Oak Ridge National Laboratory, Oak Ridge, Tennessee 37831-6422, USA*
[f]*Biosciences Division, BioEnergy Science Center, Oak Ridge National Laboratory, Oak Ridge, TN 37831, USA*
[g]*Department of Forestry, Wildlife, and Fisheries, Center for Renewable Carbon, University of Tennessee, Knoxville, TN 37996-2200, USA*

yields a racemic, cross-linked, and highly heterogeneous aromatic macromolecule.[3] The physical and chemical properties of lignin isolated from biomass depend to a large extent on its source, syringyl (S), guaiacyl (G) and *p*-hydroxyphenol (H) monomer proportions, molecular weights, degree of branching, isolation methods, and purity. Of the chemical structures in biomass lignin, guaiacyl units show a greater crosslinking reaction tendency than syringylic units,[5] which results in more condensation reactions.[3b,6] Most of the lignin generated by the Kraft pulping process and biofuel industry is currently utilized primarily as low-cost fuel.[7] Therefore, significant attention has recently turned towards the large-scale use of lignin in various applications, especially for high value-added lignin-based high performance materials. To date, the organosolv fractionation method has been widely used to isolate lignin from biomass with a number of advantages, including an efficient lignin fractionation, yielding lignin with high purity, and improved performance of the cellulose fraction in downstream conversion processes.[8] During the fractionation process, the hydrolyzed lignin is extracted into the organophilic phase and then recovered as the filtrate, leaving cellulose as a solid residue and hemicellulose fraction in the water phase as monomeric and oligomeric sugars.[9] The predominant β-O-4 ether linkages are at a lower level in organosolv lignin than the starting material due to acid-catalyzed cleavage that occurred during the organosolv process.[10] These characteristics make organosolv lignin a good candidate for high-value applications.

Lignin's syringyl/guaiacyl (S/G) monolignol ratio in biomass has been used as a good indicator of its response to pulping and biomass pretreatment.[11] In light of these correlations,[12] as well as the improved performance of engineered plastics with large amounts of guaiacyl groups,[13] this study investigates the thermal behaviour and structural changes occurring to poplar lignin with various S/G ratios under different fractionation conditions as a result of thermal treatment at various temperatures. The objective of this study is to examine the structural and fractionation parameters relevant to lignin's thermo-rheological properties and to determine how those parameters individually and cooperatively affect the melt processing of lignin as a carbon fiber precursor. Nuclear magnetic resonance (NMR) spectroscopy (*i.e.* ^{31}P NMR, HSQC NMR), gel permeation chromatography (GPC), and attenuated total reflectance (ATR) FTIR spectroscopy were employed for structural characterization. The results provide insight into lignin cross-linking and scission mechanisms under a thermo-rheological flow which might help form a basis for the potential manufacturing of lignin carbon fibers. In addition, the findings afford new insight into thermal lignin chemistry and functional group distributions that would help guide further studies into improvements in other lignin related areas, such as biomass pretreatment at elevated temperatures or generation of non-structural carbons.

Results and discussion

Lignin purity and S/G ratio

The values of the original monolignol S/G ratio in the poplar samples used in this study are shown in Table 1. After solvent fractionation of lignin from the wood samples, the S/G ratio in isolated lignin altered significantly, varying from 2.9 to 3.7, which could be attributed to the reactivity difference in the S and G units under the acidic organosolv process. The monolignol composition and S/G ratio of organosolv fractionated lignin samples are summarized in Table 2. Lignin samples from TAG896 and TAG99 that were fractionated at higher severity showed higher lignin purity at 95.30 and 94.80 wt%, respectively.

Thermal analysis

The differential scanning calorimetry (DSC) thermograms of poplar organosolv lignin samples are shown in Fig. 1.

Table 1 Syringyl/guaiacyl (S/G) ratios and chemical compositions of hybrid poplar wood (% on dry basis)

Biomass ID	S/G[a]	FC[b]	Se[c]	Ce[d]	Hm[e]	L[f]	A[g]	E[h]
TAG 1672	2.25	140 °C 120 min	1.91	42.14 ± 0.23	21.26 ± 0.08	22.63 ± 0.15	0.62 ± 0.00	7.92 ± 0.11
TAG 562	1.55	140 °C 120 min	1.91	43.55 ± 0.20	21.91 ± 0.07	22.40 ± 0.15	0.72 ± 0.02	6.17 ± 0.17
TAG 896	2.26	160 °C 60 min	2.19	42.89 ± 0.56	22.10 ± 0.22	22.22 ± 0.28	0.72 ± 0.01	6.28 ± 0.22
TAG 99	1.43	160 °C 60 min	2.19	43.79 ± 0.44	20.48 ± 0.12	22.98 ± 0.09	0.79 ± 0.01	8.01 ± 0.20

[a] S/G ratio. [b] Fractionation conditions. [c] Severity. [d] Cellulose. [e] Hemicellulose. [f] Lignin. [g] Ash. [h] Extractives.

Table 2 Lignin chemical composition with syringyl and guaiacyl contents, and S/G ratio

Biomass tag #	S[a] (%)	G[b] (%)	S/G	L[c] (wt%)	Hm[d] (wt%)
TAG1672	41.9 ± 2.1	11.9 ± 0.3	3.5 ± 0.2	91.31 ± 0.60	1.46 ± 0.10
TAG562	44.4 ± 0.1	14.2 ± 0.2	3.1 ± 0.0	91.43 ± 0.40	1.64 ± 0.34
TAG896	41.8 ± 0.2	11.9 ± 0.2	3.7 ± 0.1	95.30 ± 0.62	3.37 ± 0.07
TAG99	38.1 ± 0.6	13.3 ± 0.3	2.9 ± 0.1	94.80 ± 0.98	3.32 ± 0.03

[a] Syringyl. [b] Guaiacyl. [c] Lignin. [d] Hemicellulose.

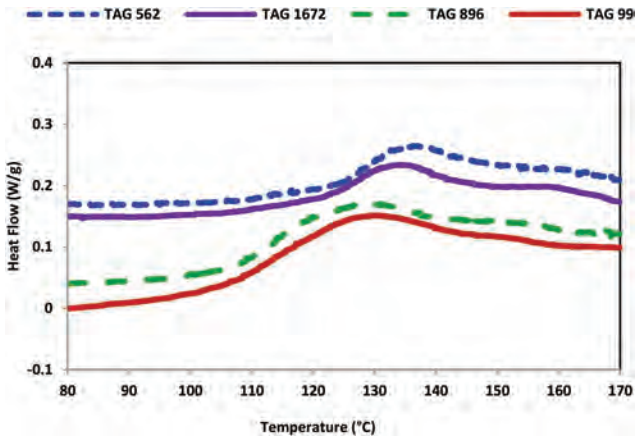

Fig. 1 DSC thermograms of poplar organosolv lignin samples showing base line shift as glass transition temperature.

It appears that the glass transition temperature (T_g) shows a broad transition range (90–140 °C) for all the analyzed lignin samples. Lignin from TAG896 with a high S/G ratio exhibits a low T_g value; in contrast, lignin from TAG562 with a low S/G ratio exhibits a higher T_g value. G moieties in poplar lignin could lead to increased crosslinking and this would impact the thermal properties of lignin. It has been reported that lignin samples with a high S and low G content would exhibit low T_g.[14] On the other hand, lignin with a high G content and low S component would exhibit high T_g.[14,15] It should be noted that TAG99 lignin also shows a low T_g value even with a low S/G ratio, which might be due to its fractionation at a higher severity.

The results from thermogravimetric analysis (TGA) of the lignin samples (preformed under a nitrogen environment) are shown in Fig. 2. The char residue at 1000 °C varies from 24–38 wt%. Lignin samples with high T_g offer higher char contents and, likewise, low T_g lignin samples have less charred residues. The TGA runs were conducted on the as-received samples without inducing any oxidative stabilization that is required for carbon fiber manufacturing. This suggests that high carbon yields might be obtained from lignins with more condensed structures. However, such a precursor is difficult to melt-spin into a fiber form.

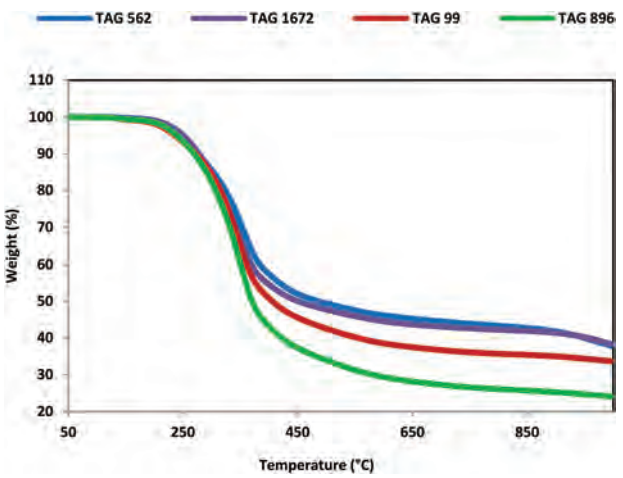

Fig. 2 TGA thermograms of isolated poplar organosolv lignin samples.

Rheological data analysis

The rheological properties of lignin play an important role in optimizing the processing conditions during the melt spinning of lignin fibers. The flow behaviours of poplar organosolv lignin samples were investigated at different temperatures of 170, 180, and 190 °C. Sample codes for the various sheared samples are shown in Table 3. As shown in Fig. 3, poplar lignin displayed differing time and temperature dependent transient viscosity profiles. The lignin samples with high T_g (*i.e.*, TAG562) exhibited higher viscosity values. Although fractionation at higher severity resulted in lower values of viscosity, lignin from TAG99 with a lower S/G ratio still exhibited relatively higher viscosity values than lignin from TAG 896 under the same fractionation conditions. Thus viscosity values appear to be controlled by both chemical reactivity as well as the degree of depolymerization of the isolated lignin. Prolonged thermo-rheological shear exposure (beyond ~20 min or 1200 s) of lignin increased the melt viscosity suggesting thermal cross-linking of lignin segments.

The melt viscosity of the lignin samples is reduced significantly with increased temperature from 170 to 190 °C. The percent increase in viscosity at high temperature (190 °C) at prolonged thermo-rheological treatment (*i.e.*, order of magnitude in $\Delta\eta$ at time lapse between 100 s and 1500 s) is very high for the lignin sample TAG562 in which the G content is relatively high. As expected, the TAG896 sample with a high S/G ratio exhibits a low viscosity at all temperature ranges and slow rise in viscosity over time. The rheo-crosslinking kinetics or chemo-rheological data analyzed based on eqn (3)–(5) are dis-

Table 3 Rheological measurement temperature and cooling conditions of poplar lignin samples and their codes

Sample code	Lignin sample	Temp. (°C)	Cooling conditions
TAG1672	Control lignin	—	—
TAG1672-170A	After rheology test	170	Air
TAG1672-180A	After rheology test	180	Air
TAG1672-190A	After rheology test	190	Air
TAG1672-190N	After rheology test	190	Nitrogen
TAG562	Control lignin	—	—
TAG562-170A	After rheology test	170	Air
TAG562-180A	After rheology test	180	Air
TAG562-190A	After rheology test	190	Air
TAG562-190N	After rheology test	190	Nitrogen
TAG896	Control lignin	—	—
TAG896-170A	After rheology test	170	Air
TAG896-180A	After rheology test	180	Air
TAG896-190A	After rheology test	190	Air
TAG896-190N	After rheology test	190	Nitrogen
TAG99	Control lignin	—	—
TAG99-170A	After rheology test	170	Air
TAG99-180A	After rheology test	180	Air
TAG99-190A	After rheology test	190	Air

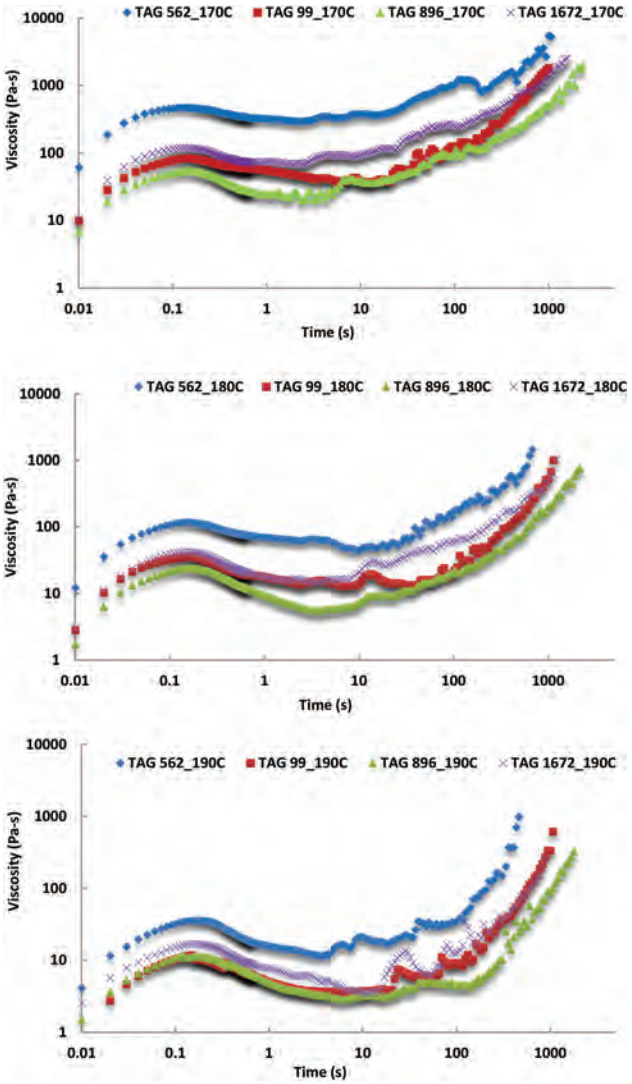

Fig. 3 Relation between the shear viscosity and shear rate of poplar lignin at different temperatures (170, 180 and 190 °C).

played in Table 4. The equilibrium rate constants (k_∞) for the thermo-chemical reactions of lignins from TAG896 and TAG99 are significantly lower than the other samples, since both these samples were obtained under high severity conditions (high temperature) and have very low T_g compared to others. Although the TAG99 sample has a relatively lower S content than the other lignins, the high severity extraction conditions could be the reason for its anomalous reactivity. The activation energy for the thermal reactions ($\Delta E_k/R$) follows a similar trend to that of the equilibrium rate constant (k_∞). The activation energy ($\Delta E_{\dot{E}}/R$) is relatively higher for organosolv lignin TAG1672 as compared to lignin samples from TAG896, TAG562 and TAG99.

Table 4 Chemo-rheological characteristics of poplar lignin

Sample ID	k_∞ (1/s)	η_∞ (Pa s)	$\Delta E_k/R$ (K)	$\Delta E_{\dot{E}}/R$(K)
TAG1672	4.5×10^7	1.14×10^{-31}	−10 685	34 028
TAG562	4.4×10^8	6.48×10^{-26}	−11 472	28 409
TAG896	74	2.58×10^{-27}	−4709	29 059
TAG99	43	4.19×10^{-27}	−4181	28 865

Molecular weight analysis

GPC was employed to determine the molecular weight distribution of poplar organosolv lignin before and after rheology testing. The weight-averaged molecular weight (M_w) and number-averaged molecular weight (M_n) values for the lignin samples are presented in Fig. 4. Compared with the controls, lignin molecular weights increased to different extents after rheological testing at 170 °C. As the temperature increased to 190 °C, the lignin molecular weights were observed to decrease. This decrease corresponds to their viscosity properties and suggests that most of the repolymerization reactions in lignin occur at lower processing temperatures, since the depolymerization of lignin dominates at higher temperatures.[16] The significant increase of molecular weight in TAG562 lignin after the rheology test at 170 °C in conjunction with its higher viscosity values suggests that lignin with a lower S/G ratio could result in the condensation reaction to occur to a higher extent. The organosolv lignins from TAG99 and TAG896 have lower molecular weights than the other lignin samples, because those two samples were isolated at higher severity of organosolv fractionation which could lead to a decrease in lignin molecular weights due to enhanced hydrolysis of lignin.[17] TAG99 lignin with a low S/G ratio is significantly depolymerized (likely this is why it exhibits a low T_g

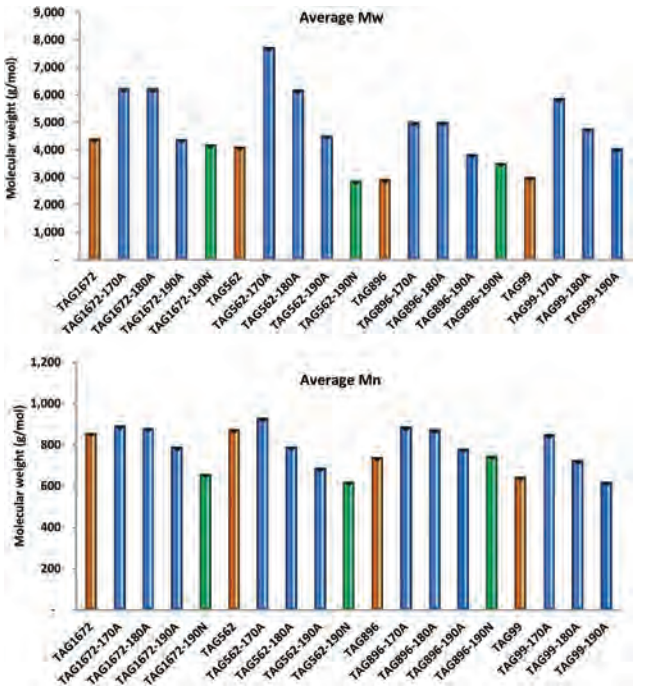

Fig. 4 Molecular weights of lignins after the rheology test. Sample code with definition is in Table 3.

value) and thus it behaves differently in the rheological response discussed earlier. Viscosity typically depends on molecular weights and in some cases its change depends, in part, on chemical reactivity. These two combined effects give TAG99 lignin moderate viscosity behavior and a low rate constant value (k_∞ in Table 4). In addition, lignin samples cooled under air after the 190 °C rheology test exhibited higher molecular weights than those under nitrogen. This suggests that oxygen during cooling could affect the lignin macromolecular structure and contributes more to the formation of repolymerized structures in comparison to nitrogen.[18]

NMR and FTIR analysis

^{31}P NMR, ^{1}H-^{13}C HSQC NMR, and ATR-FTIR spectroscopies were employed to investigate structural changes occurring in poplar organosolv lignins as a result of the thermal rheology treatment. Lignin phosphitylation and ^{31}P NMR quantitative analysis was carried out to analyze the amounts and distribution of various hydroxyl structures as summarized in Fig. 5. Compared to control samples before rheology treatment, there is a reduction in the aliphatic hydroxyl group contents in lignin. The decreased amounts of these hydroxyl groups indicate that lignin side chain hydroxyl groups were eliminated under the applied thermal conditions, especially at a high temperature of 190 °C. The cleavages of side chain hydroxyl groups could be attributed to the dehydration of aliphatic hydroxyl groups yielding sites of unsaturation and/or new formed cross-linkages bridging the aromatic rings. The carboxylic OH group contents also decrease as the rheology testing temperature is raised from 170 to 190 °C. Guaiacyl and syringyl type phenolic hydroxyl group contents were observed to increase after the rheology treatment at 170 °C (TAG1672, TAG562 and TAG896) which could result from the cleavage of ether bonds. The decrease of ether linkages was further confirmed by ATR-FTIR semi-quantitative analysis of main ether linkages as shown in Fig. 6. However, rheology treatment at higher temperature (190 °C) yielded lower amounts of phenolic OH groups, which could be attributed to the intensive elimination reactions that transformed hydroxyl groups to water and double bonds.

In addition, ^{31}P NMR analysis shows noticeably increased amounts of C5 condensed phenolic structures in poplar organosolv lignin after 170 °C rheology treatment. This suggests that rheology testing at 170 °C could lead to lignin repolymerization, thereby resulting in modified lignin with higher viscosity and molecular weights, consistent with GPC results with respect to the increase of related molecular weights. In contrast, the higher temperature of 190 °C tends to favor depolymerization of lignin to a large degree, thereby generating lignin with lower molecular weights and lower viscosity. During rheology testing, lignin with a lower S/G ratio generates more cross-linkages that could exist as a bridge between the aromatic rings and/or as a cyclic form attached to aromatic carbons. This could be attributed to the active phenyl C5 site of guaiacyl units resulting in cross-linking reactions in a higher proportion for guaiacyl lignins. Moreover, a large amount of aliphatic OH in the TAG562 control organosolv lignin sample would be another key factor affecting their molecular weight and viscosity increase during the rheology test, because the strength of hydrogen bonding for primary *versus*

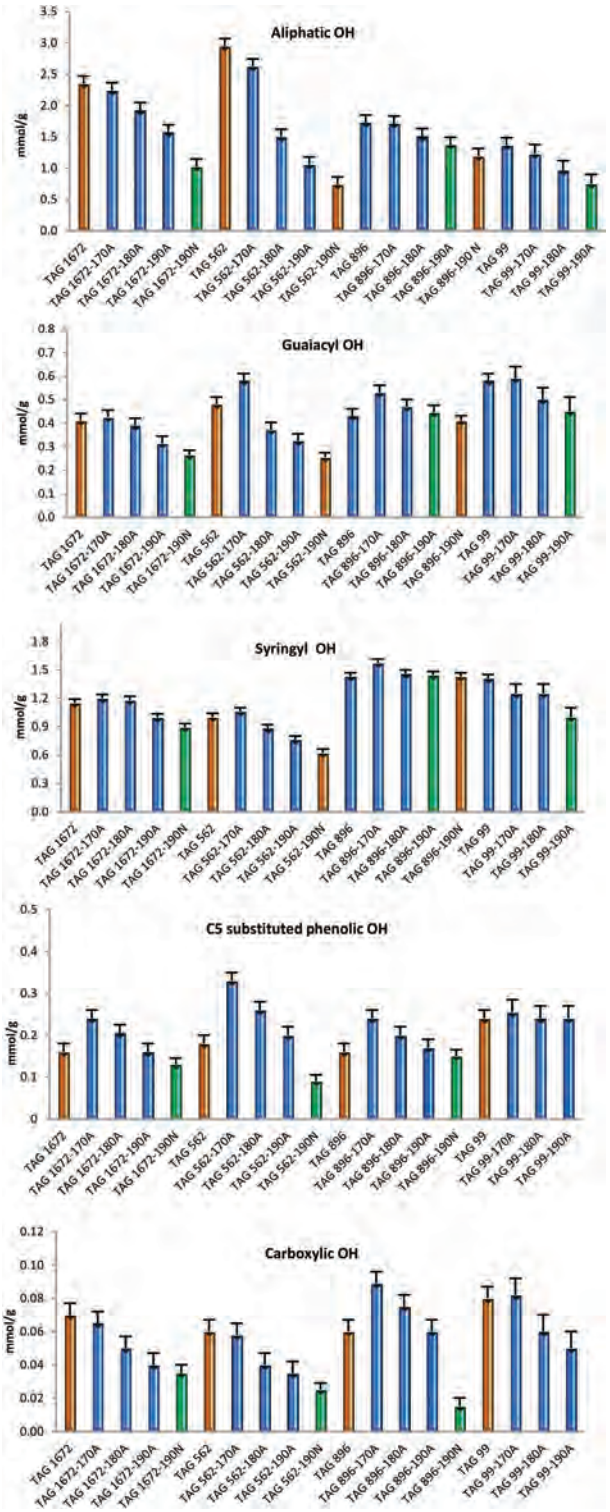

Fig. 5 Hydroxyl contents in lignin determined by using ^{31}P NMR. Sample code with definition is in Table 3.

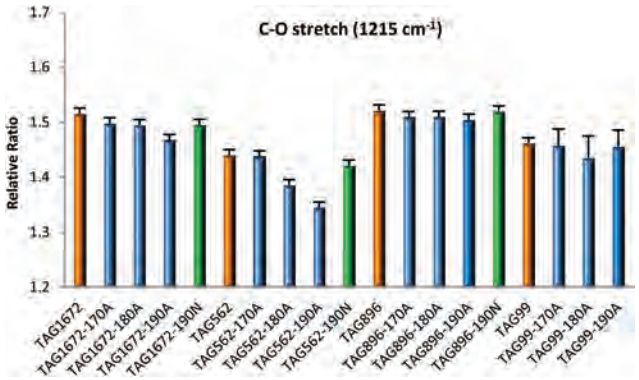

Fig. 6 Ether linkages' relative ratio calculated from ATR-FTIR absorption data. Sample code with definition is in Table 3.

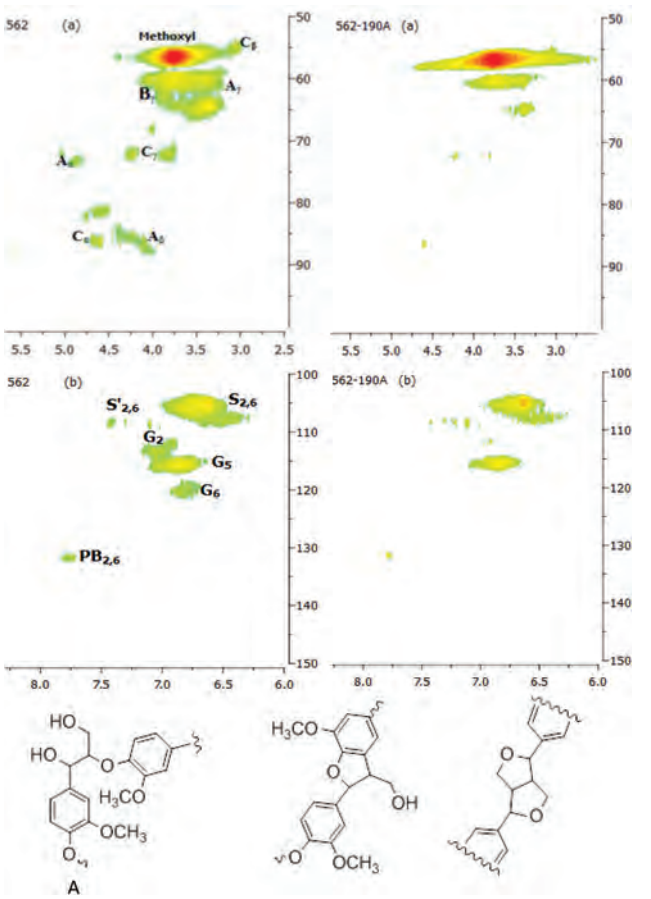

Fig. 7 HSQC spectra of TAG562 poplar organosolv lignin after rheology treatment. (a) Aliphatic region; (b) aromatic region; A: β-O-4 ether; B: phenyl coumaran; C: resinol; G: guaiacyl; S: syringyl; S′: syringyl units with oxidized α-ketone; PB: *p*-hydroxybenzoate.

secondary alcohols is different. A previous study has shown that the presence of γ-OH groups strongly reduced the thermal mobility of the β-O-4 model oligomers.[19] Therefore, lignin containing more aliphatic OH groups including both secondary α-OH and primary γ-OH groups would be shown to be more infusible during the rheology test. Moreover, thermally treated lignin samples acquired under nitrogen cooling after the rheology test at 190 °C yielded smaller amounts of various hydroxyl groups than lignin under air cooling, which indicates that oxygen could oxidize lignin and introduce more oxygenated compounds into the lignin macromolecules.

In an effort to further investigate changes in the lignin chemical structure during rheological treatment at 190 °C, HSQC NMR of three groups of lignin were carried out. Fig. 7 shows the HSQC spectra for the TAG562 organosolv lignin sample before and after rheological treatment at 190 °C under air cooling. The cross peaks were assigned by comparing with the literature data.[20] HSQC spectra show a significant reduction in the signal intensity of cross peaks in inter-unit linkages, indicating the scission of ether linkages during rheology treatment. In agreement with changes in the aliphatic region, there is also a considerable reduction in aromatic resonances including syringyl and guaiacyl lignin units after the rheology treatment at 190 °C, indicating the change of lignin side chains and possible repolymerization reaction of aromatic units. Interestingly, lignin under nitrogen cooling remained with relatively more β-O-4 ether linkages than lignin under air cooling. This could suggest that nitrogen's inert properties could protect lignin thus resulting in a smaller scission of ether linkages at the temperature of 190 °C. This in conjunction with the molecular weight; ^{31}P NMR, and FTIR results indicate that oxygen (*i.e.*, O_2) could contribute to the formation of cross-linkages among lignin molecules through a series of elimination, rearrangement and oxidative reactions of free radicals derived from the homolysis of β-O-4 ether bonds in lignin.

Furthermore, the possible mechanistic pathways associated with these structural changes during thermal rheology testing that resulted in heat-induced polymerization and depolymerization of lignin are proposed in Scheme 1. At relatively low temperature, lignin samples could be mainly subjected to repolymerization reactions starting from the initial homolysis of C_α and/or C_β-ether linkages (A in Scheme 1) generating a phenoxyl (C) and 1-phenyl-2-propyl (B) radical.[21] The formed phenoxyl radical with the resonance mesomeric forms (C1) leads to radical coupling reactions with C5 and/or C3 centered radicals to form new 4-O-5, 5-5′, 3-3′, 3-5′ and 3-O-5 linkages along with increased molecular weight and condensed lignins. This suggests lignin with more guaiacyl (G) units could result in more cross-linkages due to less steric hindrance in the lignin C5 position that facilitates the formation of resonance structures. At a relatively high temperature (during the rheology test of lignin), the polymer undergoes competitive repolymerization and depolymerization reactions, and the depolymerization reaction appears to be dominant as evident by the apparent decrease in molecular weight and hydroxyl groups in lignin.[16] Radical induced H-abstraction occurring at the C_α–H could form a benzyl radical that should have a lower unpaired spin density at the α-position with extensive electron delocalization analogous to the formed phenoxyl radicals.[16] Two different pathways for depolymerization reaction thus

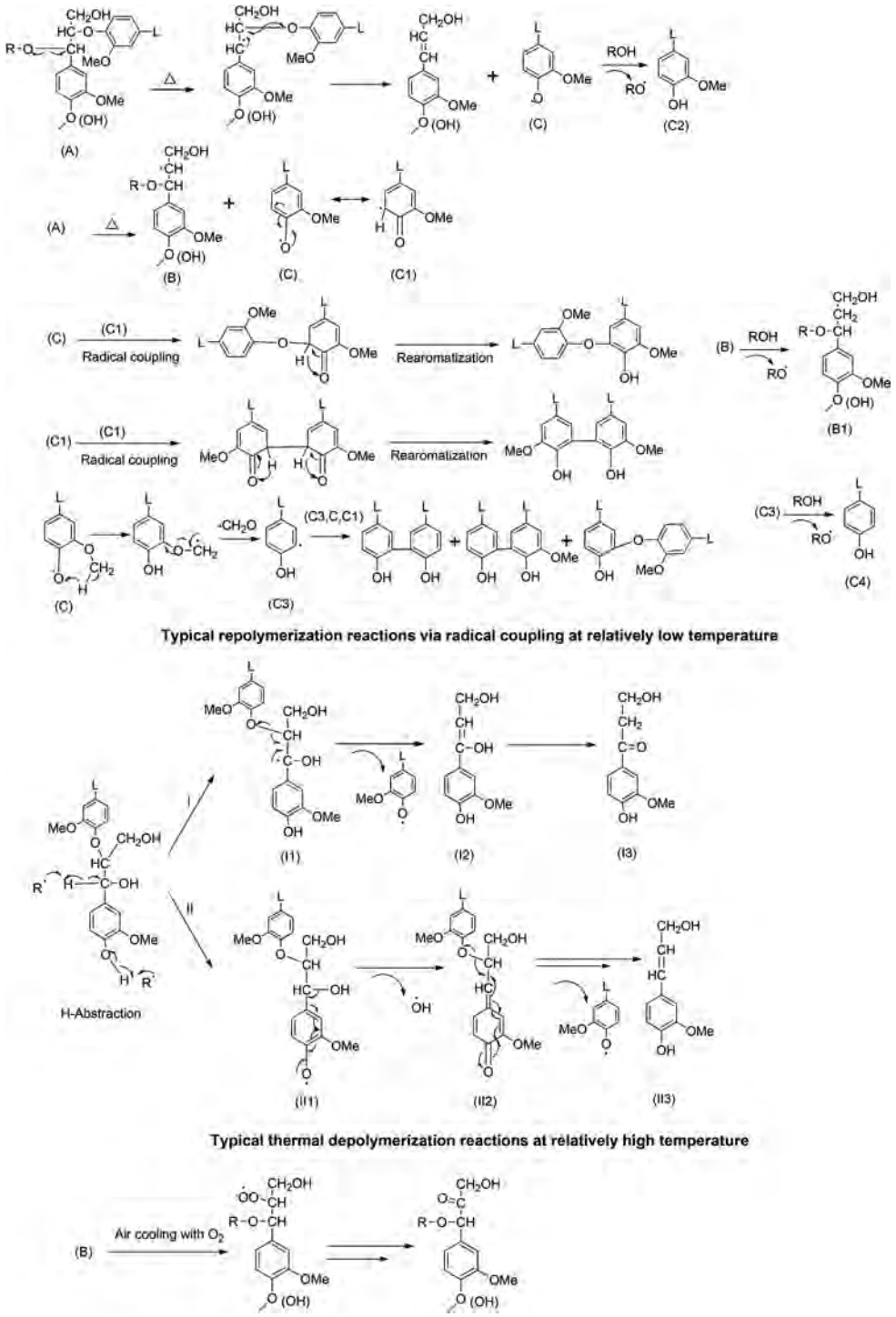

Scheme 1 Proposed lignin repolymerization and depolymerization reaction mechanisms during melt rheology treatment.

could be proposed in order to not only control molecular weight growth but also transform the reactive C–O bonds into C–C linkages. The 1-phenyl-2-propyl radical (B) formed at relatively low temperature is reported to be more exothermic than that of the phenoxyl radical.[21a] Although intermediates generated by those radicals would be sterically hindered which further limit their participation in the chain propagating reaction, these radicals could be severely limited with regard to the sites that are capable of abstracting hydrogen from lignin to form more stable intermediates for depolymerization reactions (possible pathways I and II in Scheme 1) at relatively high temperature. Furthermore, cooling under air will lead to a series of highly reactive oxygen-based radicals, which further oxidizes the lignin structure introducing more carbonyl and

carboxyl groups into lignin than under nitrogen cooling conditions.[16]

Conclusions

A rheology test of organosolv lignins from poplar with different S/G ratios was accomplished at 170, 180, and 190 °C under different cooling conditions. At 170 °C, repolymerization of lignin is favored, which resulted in the significant increase in molecular weights and viscosity values. In contrast, at 190 °C lignin depolymerization appears to be dominant as exhibited by a considerable reduction of β-O-4 ether linkages, aliphatic, phenolic and carboxylic hydroxyls, and therefore yielded lignins with relatively lower molecular weights and lower viscosity values. Air cooling introduced more oxygenated compounds and condensed bonds into the lignin macromolecules but lower amounts of ether linkages than nitrogen cooling. Poplar organosolv lignins with a lower S/G ratio exhibited higher viscosity values and molecular weights with larger amounts of condensed structures after the rheology test at relatively lower temperature. Suitable temperature and air cooling conditions could contribute to the crosslinking of lignin and the formation of condensed structures with more carbon–carbon linkages that improve the spinnability of organosolv poplar lignins. The detailed characterization of lignin physicochemical properties after rheology treatment provides insight into the mechanisms of rheology of lignin and will be of value in the production of novel lignin carbon fibers. A further study using bench scale lignin samples to synthesize carbon fibers containing such treated lignin will be needed in the future for efficiently incorporating lignin in carbon fiber production.

Experimental

Biomass and lignin isolation

Three-year-old black cottonwood (*Populus trichocarpa*) clones harvested from a Genome-wide Association Study at Clatskanie, OR were harvested Dec. 2012, cut into ~50 cm logs and shipped to ORNL, where they were dried for 2 weeks at 70 °C. The logs were then debarked with an axe and an angle grinder and then chipped to ~1–3 cm sections in a commercial chipper. A small amount of the chips were ground to 0.420 mm and the powder samples were analyzed by pyrolysis molecular-beam mass spectrometry (py-MBMS) to determine the S/G ratio. Four trees with S/G ratio ranging from 1.43 to 2.26 were selected to perform organosolv fractionation process. Poplar clone identification codes for selected samples are shown in Table 1. The chemical composition of the biomass samples was determined by following procedures developed by National Renewable Energy Laboratory (NREL/TP-510-42619, NREL/TP-510-42618 and NREL/TP-510-42622). The ash, extractives, cellulose, hemicellulose, and lignin content of the poplar samples are summarized in Table 1. The selected hybrid poplar wood chips were sieved and particles with size larger than 2.36 mm were placed in a flow through reactor and heated with a mixture of methyl isobutyl ketone/ethanol/water (16/34/50 wt%) in presence of sulfuric acid (0.05 M).[10c] The organosolv fractionation process was carried out at 140 °C for 120 min or 160 °C for 60 min with solid to liquid loading ratio 1 : 20 (w/w). The combined severity factor (Ro′) of the fractionation, which combines the effects of reaction time, temperature, and acid concentration into a single value, was calculated as follows:[22]

$$\mathrm{Ro}' = \log \mathrm{Ro} - \mathrm{pH} \quad (1)$$

$$\mathrm{Ro} = (t)\ (\exp(T_\mathrm{r} - T_\mathrm{b})/14.75) \quad (2)$$

where t represents fractionation time in minutes; T_r is the fractionation temperature in °C; T_b is the baseline temperature, mostly at 100 °C. After the organosolv process, lignin was isolated from the resulting cooking liquor by a reported salting-out method.[10c,23]

Lignin characterization and thermal analysis

The lignin samples were characterized by using pyrolysis-gas chromatography/mass spectrometry. Briefly, 200 μg of lignin were pyrolyzed in a Frontier multi-shot pyrolyzer (PY3030D) at 450 °C for 12 s. The interface temperature was 280 °C. A Perkin Elmer Clarus 680 GC with a split ratio of 80 : 1 was used for compound separation. The sample was injected into a 30 m × 0.25 i.d. × 0.25 μm Elite 1701 (Perkin Elmer) capillary column with 1 mL min^{-1} helium gas. A Perkin Elmer Clarus SQ8C mass spectrometer with a scanning range of 35–550 Da was used to detect the eluting component. The S and G % of lignin fractions were calculated following the method developed by Sykes *et al.*[24] Thermal analysis of the lignin samples was conducted in a TA Q500 thermogravimetric analyzer (TGA) heated from RT (30 °C) to 1000 °C, at 10 °C min^{-1} under a nitrogen atmosphere. Differential scanning calorimetry (DSC) was carried out on lignin samples using a TA Instruments DSC Q2000 in standard mode. Second heating scans ran at 10 °C min^{-1} was used to determine the glass transition temperature of the lignin samples.

Rheological measurement

The melt viscosity values of the lignin samples (~400 mg) were measured using a strain-controlled ARES rheometer (TA Instruments). Isothermal transient rheological analysis was conducted using parallel plate geometry (25 mm diameter plate) at three temperatures (170, 180, and 190 °C) with a 1 mm gap and a shear rate of 10 rad s^{-1}. Parallel aluminium plates were first heated to the desired temperature at a ramp rate of 5 °C min^{-1}. Once the desired temperature was reached, nitrogen gas was purged through the oven. The lignin was compressed into a pellet and loaded after the reset of the gap and forced between the upper and lower plate. The upper plate was gradually lowered to contact the lignin sample, finally to reach a 1 mm gap. The lignin sample was isothermally sheared in between the preheated parallel plate at a constant shear rate

(10 rad s^{-1}) and viscosity data were monitored at 170, 180, and 190 °C under nitrogen during the rheological test (for ~2000 s), and then cooled down to room temperature under air or nitrogen environments (by purging room temperature air or nitrogen, respectively) in approximately 1 h, separately. Sample codes for the various sheared lignin samples are shown in Table 3. The recorded data showed a short duration (10–200 s) of steady viscosity after a short increase at the beginning of measurement of transient data; then the viscosity increases due to thermally-induced reactions. The gradual increase in viscosity data was analysed by fitting eqn (3)–(5).

$$\ln \eta(t) = \ln \eta_\gamma + kt \quad (3)$$

$$\eta_\gamma = \eta_\infty \exp\left(\frac{\Delta E_\eta}{RT}\right) \quad (4)$$

$$k = k_\infty \exp\left(\frac{\Delta E_k}{RT}\right) \quad (5)$$

Eqn (3) shows k as the temperature dependent reaction rate constant and η_γ as the steady viscosity value at the onset of viscosity rise. Chemorheological activation energies associated with the temperature dependence of viscosity (ΔE_η) and rate constants (ΔE_k) were studied using isothermal viscosity data and fitting eqn (4) and (5).[25]

ATR-FTIR analysis

To investigate and semi-quantify chemical changes in lignin after rheological treatment, a PerkinElmer Spectrum 100 FTIR spectrometer with a universal ATR sampling accessory was used. The lignin sample was pressed uniformly against the crystal surface *via* a spring-anvil, and the spectrum was obtained by accumulating 32 scans from 4000 to 500 cm^{-1} at 4 cm^{-1} resolution. An ATR correction and baseline correction were carried out by using PerkinElmer Spectrum software. Semi-quantitative analysis of chemical group change was carried out by normalizing the FTIR absorption spectra at a band position of 1506 cm^{-1} representing lignin aromatic skeletal vibration based on related studies.[26]

Gel permeation chromatography (GPC) analysis

The lignin samples after rheological treatment (dried under vacuum at 40 °C overnight) were acetylated with acetic anhydride/pyridine (1/1, v/v) at RT for 24 h in a sealed flask under an inert atmosphere. The concentration of the lignin in the solution was approximately 20 mg mL^{-1}. After 24 h, the solution was diluted with ~20 mL of ethanol and stirred for an additional 30 min, after which the solvents were removed with a rotary evaporator followed by drying in a vacuum oven at 40 °C. Prior to GPC analysis the acetylated lignin sample was dissolved in tetrahydrofuran (1.0 mg mL^{-1}), filtered through a 0.45 μm filter, and placed in a 2 mL auto-sampler vial. The molecular weight distributions of the acetylated lignin samples were then analyzed on an Agilent GPC SECurity 1200 system equipped with four Waters Styragel columns (HR1, HR2, HR4, HR6), an Agilent refractive index (RI) detector, and an Agilent UV detector (270 nm), using tetrahydrofuran (THF) as the mobile phase (1.0 mL min^{-1}), with an injection volume of 20.0 μL. A standard polystyrene sample was used for calibration. The number-average molecular weight (M_n) and weight-average molecular weight (M_w) were determined by GPC. Average data of M_w, M_n and polydispersity index (PDI) were presented based on three different rheology tests on each poplar lignin sample at different temperatures.

Quantitative ^{31}P-NMR analysis

Lignin phosphitylation and ^{31}P-NMR analysis was used to quantitatively determine hydroxyl functional groups in lignin samples. Quantitative ^{31}P-NMR spectra were acquired after *in situ* derivatization of the lignin sample using about 15.0 mg of the lignin sample with 2-chloro-4,4,5,5-tetramethyl-1,3,2-dioxaphospholane (TMDP) in a solution of (1.6 : 1, v/v) pyridine/$CDCl_3$ containing chromium acetylacetonate (relaxation agent) and *endo-N*-hydroxy-5-norbornene-2,3-dicarboximide (NHND, internal standard). ^{31}P NMR analysis of lignin samples was carried out using a Bruker Avance 400 MHz NMR spectrometer operating at frequencies of 161.93 MHz for ^{31}P at 25 °C in a magnetic field of 9.4 Tesla. The quantitative ^{31}P NMR spectra were acquired using an inverse gated decoupling pulse sequence with a 25 s pulse delay and 128 scans. The average data of lignin functional groups were presented based on three repeated rheology tests on each poplar lignin sample at various temperatures.

Heteronuclear single quantum coherence (HSQC) NMR analysis

HSQC experiments of lignin after rheological treatment were carried out using a Bruker Avance 400 MHz NMR spectrometer. NMR samples were prepared as follows: 50 mg of the lignin sample was added to 0.5 mL deuterated hexamethylphosphoramide (HMPA-d_{18}) and stirred at 45 °C for 4 hours. A standard Bruker pulse sequence with 13 ppm spectra width in F2 (^{1}H) dimension with 1024 data points (95.9 ms acquisition time), 210 ppm spectra width in F1 (^{13}C) dimension with 256 data points (6.1 ms acquisition time), a 90° pulse, 1.5 s pulse delay, $^1J_{C-H}$ of 145 Hz and 48 scans was employed. NMR data were processed using the TopSpin 2.1 software (Bruker BioSpin) and MestreNova (Mestre Labs) software packages.

Acknowledgements

Part of the research was sponsored by the Laboratory Directed Research and Development Program of Oak Ridge National Laboratory (ORNL), managed by UT-Battelle, LLC, for the U.S. Department of Energy. This work was also supported and performed as part of the BioEnergy Science Center. The BioEnergy Science Center is a U.S. Department of Energy Bioenergy Research Center supported by the Office of Biological and Environmental Research in the DOE Office of Science. The Georgia Tech authors also acknowledge the financial support from the paper science engineering (PSE) fellowship program

in Renewable Bioproducts Institute at Georgia Institute of Technology.

This manuscript has been authored by UT-Battelle, LLC under Contract No. DE-AC05-00OR22725 with the U.S. Department of Energy. The United States Government retains and the publisher, by accepting the article for publication, acknowledges that the United States Government retains a non-exclusive, paid-up, irrevocable, world-wide license to publish or reproduce the published form of this manuscript, or allow others to do so, for United States Government purposes. The Department of Energy will provide public access to these results of federally sponsored research in accordance with the DOE Public Access Plan (http://energy.gov/downloads/doe-public-access-plan).

Notes and references

1 S. Chand, *J. Mater. Sci.*, 2000, **35**, 1303–1313.
2 (*a*) T. Saito, R. H. Brown, M. A. Hunt, D. L. Pickel, J. M. Pickel, J. M. Messman, F. S. Baker, M. Keller and A. K. Naskar, *Green Chem.*, 2012, **14**, 3295–3303; (*b*) A. Awal and M. Sain, *J. Appl. Polym. Sci.*, 2013, **129**, 2765–2771.
3 (*a*) P. Sannigrahi, Y. Pu and A. Ragauskas, *Curr. Opin. Env. Sust.*, 2010, **2**, 383–393; (*b*) J. Ralph, K. Lundquist, G. Brunow, F. Lu, H. Kim, P. F. Schatz, J. M. Marita, R. D. Hatfield, S. A. Ralph and J. H. Christensen, *Phytochem. Rev.*, 2004, **3**, 29–60.
4 (*a*) D. A. Baker and T. G. Rials, *J. Appl. Polym. Sci.*, 2013, **130**, 713–728; (*b*) H. Mainka, L. Hilfert, S. Busse, F. Edelmann, E. Haak and A. S. Herrmann, *J. Mater. Res. Technol.*, 2015, **4**, 377–391.
5 (*a*) I. Norberg, Y. Nordström, R. Drougge, G. Gellerstedt and E. Sjöholm, *J. Appl. Polym. Sci.*, 2013, **128**, 3824–3830; (*b*) M. Foston, G. A. Nunnery, X. Meng, Q. Sun, F. S. Baker and A. Ragauskas, *Carbon*, 2013, **52**, 65–73.
6 Q.-N. Sun, T.-F. Qin and G.-Y. Li, *Int. J. Polym. Anal. Charact.*, 2009, **14**, 19–33.
7 A. J. Ragauskas, C. K. Williams, B. H. Davison, G. Britovsek, J. Cairney, C. A. Eckert, W. J. Frederick, J. P. Hallett, D. J. Leak and C. L. Liotta, *Science*, 2006, **311**, 484–489.
8 (*a*) M. Oliet, J. Garcıa, F. Rodrıguez and M. Gilarrranz, *Chem. Eng. J.*, 2002, **87**, 157–162; (*b*) A. A. Shatalov and H. Pereira, *Carbohydr. Polym.*, 2007, **67**, 275–281; (*c*) H. Sixta, H. Harms, S. Dapia, J. Parajo, J. Puls, B. Saake, H.-P. Fink and T. Röder, *Cellulose*, 2004, **11**, 73–83.
9 X. Pan, J. F. Kadla, K. Ehara, N. Gilkes and J. N. Saddler, *J. Agric. Food Chem.*, 2006, **54**, 5806–5813.
10 (*a*) R. El Hage, N. Brosse, L. Chrusciel, C. Sanchez, P. Sannigrahi and A. Ragauskas, *Polym. Degrad. Stab.*, 2009, **94**, 1632–1638; (*b*) P. Sannigrahi, A. J. Ragauskas and S. J. Miller, *Energy Fuels*, 2010, **24**, 683–689; (*c*) J. J. Bozell, C. O'Lenick and S. Warwick, *J. Agric. Food Chem.*, 2011, **59**, 9232–9242.
11 P. Sannigrahi, A. J. Ragauskas and G. A. Tuskan, *Biofuels, Bioprod. Biorefin.*, 2010, **4**, 209–226.
12 (*a*) G. Papa, P. Varanasi, L. Sun, G. Cheng, V. Stavila, B. Holmes, B. A. Simmons, F. Adani and S. Singh, *Bioresour. Technol.*, 2012, **117**, 352–359; (*b*) F. Guo, W. Shi, W. Sun, X. Li, F. Wang, J. Zhao and Y. Qu, *Biotechnol. Biofuels*, 2014, **7**, 38; (*c*) B. H. Davison, S. R. Drescher, G. A. Tuskan, M. F. Davis and N. P. Nghiem, in *Twenty-Seventh Symposium on Biotechnology for Fuels and Chemicals*, Springer, 2006, pp. 427–435.
13 (*a*) H. Hatakeyama and T. Hatakeyama, in *Biopolymers*, Springer, 2010, pp. 1–63; (*b*) S. Kubo and J. F. Kadla, *Macromolecules*, 2004, **37**, 6904–6911.
14 A. Olsson and L. Salmén, in *ACS symposium series (USA)*, 1992, 489, pp. 133–143.
15 (*a*) A. Tejado, C. Pena, J. Labidi, J. Echeverria and I. Mondragon, *Bioresour. Technol.*, 2007, **98**, 1655–1663; (*b*) N. E. El Mansouri, Q. Yuan and F. Huang, *BioResources*, 2011, **6**, 2647–2662.
16 J. Braun, K. Holtman and J. Kadla, *Carbon*, 2005, **43**, 385–394.
17 R. El Hage, N. Brosse, P. Sannigrahi and A. Ragauskas, *Polym. Degrad. Stab.*, 2010, **95**, 997–1003.
18 K. Sudo and K. Shimizu, *J. Appl. Polym. Sci.*, 1992, **44**, 127–134.
19 Y. Uraki, Y. Sugiyama, K. Koda, S. Kubo, T. Kishimoto and J. F. Kadla, *Biomacromolecules*, 2012, **13**, 867–872.
20 (*a*) H. L. Trajano, N. L. Engle, M. Foston, A. J. Ragauskas, T. J. Tschaplinski and C. E. Wyman, *Biotechnol. Biofuels*, 2013, **6**, 110; (*b*) Y. Pu, F. Chen, A. Ziebell, B. H. Davison and A. J. Ragauskas, *BioEnergy Res.*, 2009, **2**, 198–208.
21 (*a*) T. Elder, *Holzforschung*, 2010, **64**, 435–440; (*b*) C. Cui, H. Sadeghifar, S. Sen and D. S. Argyropoulos, *BioResources*, 2013, **8**, 864–886; (*c*) T. Nakamura, H. Kawamoto and S. Saka, *J. Anal. Appl. Pyrolysis*, 2008, **81**, 173–182; (*d*) H. Kawamoto, T. Nakamura and S. Saka, *Holzforschung*, 2008, **62**, 50–56.
22 (*a*) H. L. Chum, D. K. Johnson and S. K. Black, *Ind. Eng. Chem. Res.*, 1990, **29**, 156–162; (*b*) R. Overend, E. Chornet and J. Gascoigne, *Philos. Trans. R. Soc., A*, 1987, **321**, 523–536; (*c*) M. Pedersen and A. S. Meyer, *New Biotechnol.*, 2010, **27**, 739–750.
23 J. J. Bozell, S. K. Black, M. Myers, D. Cahill, W. P. Miller and S. Park, *Biomass Bioenergy*, 2011, **35**, 4197–4208.
24 R. Sykes, M. Yung, E. Novaes, M. Kirst, G. Peter and M. Davis, in *Biofuels: Methods and Protocols*, Springer, 2009, pp. 169–183.
25 M. J. Bortner, V. Bhanu, J. E. McGrath and D. G. Baird, *J. Appl. Polym. Sci.*, 2004, **93**, 2856–2865.
26 (*a*) S. Kubo and J. F. Kadla, *Biomacromolecules*, 2005, **6**, 2815–2821; (*b*) G. Hu, C. Cateto, Y. Pu, R. Samuel and A. J. Ragauskas, *Energy Fuels*, 2011, **26**, 740–745; (*c*) Q. Sun, M. Foston, X. Meng, D. Sawada, S. V. Pingali, H. M. O'Neill, H. Li, C. E. Wyman, P. Langan and A. J. Ragauskas, *Biotechnol. Biofuels*, 2014, **7**, 150.

